Experimental rat model for cervical compressive myelopathy

Yasushi Ijima[a], Takeo Furuya[a], Masao Koda[c], Yusuke Matsuura[a], Junya Saito[a], Mitsuhiro Kitamura[a], Takuya Miyamoto[a], Sumihisa Orita[a], Kazuhide Inage[a], Takane Suzuki[b], Masashi Yamazaki[c] and Seiji Ohtori[a]

Previously, a rat model of chronic compressive myelopathy that uses a water-absorbing polymer inserted under a spinal lamina was reported. However, the best size and coefficient of expansion of the polymer sheet have not yet been established. The aim of the present study was to optimize these properties in an ideal rat model of cervical compressive myelopathy. Thirty rats were used in this study. A sheet of water-absorbing polymer was inserted under the cervical laminae. Rats were divided randomly into five experimental groups by the expansion rate (350 or 200%) and thickness (0.5 or 0.7 mm) and the control. After the surgery, the severity of paralysis was evaluated for 12 weeks. At 12 weeks after the surgery, cresyl violet staining was performed to assess the number of motor neurons in the anterior horn at the C4/C5 segment and Luxol Fast Blue staining was performed to assess demyelination in the corticospinal tract at the C7 segment. 'Slow-progressive' paralysis appeared at 4–8 weeks postoperatively in rat models using sheets with 200% expansion. By contrast, only temporary paralysis was observed in rat models using sheets with 350% expansion. A loss of motor neurons in the anterior horn was observed in all groups, except for the control. Demyelination in the corticospinal tract was observed in rat models using sheets with 200% expansion, but not rat models using sheets with 350% expansion. A polymer sheet that expands its volume by 200% is an ideal material for rat models of cervical compressive myelopathy. *NeuroReport* **28:1239–1245**

NeuroReport 2017, **28:**1239–1245

Keywords: cervical compressive myelopathy, chronic, rat model

Departments of [a]Orthopedic Surgery, [b]Environmental Medicine, Chiba University Graduate School of Medicine, Chiba and [c]Department of Orthopedic Surgery, University of Tsukuba, Tsukuba, Japan

Correspondence to Takeo Furuya, MD, PhD, Department of Orthopedic Surgery, Chiba University Graduate School of Medicine, 1-8-1 Inohana, Chuo-Ku, Chiba 2608677, Japan
Tel: +81 43 226 2961; fax: +81 43 224 5124; e-mail: furuya-takeo@chiba-u.jp

Received 6 August 2017 **accepted** 31 August 2017

Introduction

Cervical compressive myelopathy (CCM) is a common cause of neurological disability.

Chronic spinal cord compression is mainly caused by chronic degenerative changes in the cervical spine, disk herniation, ossification of the posterior longitudinal ligament, and ossification of the ligamentum flavum, resulting in slowly progressive impairment in motor and sensory functions of the limbs [1–3]. Currently, surgical decompression can attenuate the progression of CCM, but most patients are still left with significant neurological impairment [4]. No effective pharmacological treatment is available to improve neurological disability in patients with postoperative persistence of neurological deficits and patients who are unable to tolerate surgical treatment. The detailed pathophysiological mechanisms of CCM are poorly understood.

Previously described animal models of CCM are mostly a replacement of acute compression methods using impactors such as the Infinite Horizon impactor and the New York University impactor [5]. Few reports are available on animal models of 'chronic' or 'slow-progressive' compressive myelopathy. Kim *et al.* [6] and Long *et al.* [7] reported a rat model of chronic compressive myelopathy that uses a water-absorbing polymer sheet inserted under a spinal lamina. Kim *et al.* [6] used a sheet measuring 0.7 mm × 3 mm × 5 mm that expands in volume by 230%. By contrast, Long *et al.* [7] used a sheet measuring 1 mm × 3 mm × 1 mm that expands in volume by 700%. The optimal size and coefficient of expansion of the polymer sheet have not yet been established. The aim of the present study was to optimize these properties in an ideal rat model of CCM using a water-absorbing polymer sheet.

Materials and methods

Surgical procedure

We used 30 eight-week-old female Sprague-Dawley rats in the present study. Rats were anesthetized with sevoflurane and fixed in a prone position. An incision was

0959-4965 Copyright © 2017 The Author(s). Published by Wolters Kluwer Health, Inc. DOI: 10.1097/WNR.0000000000000907

Fig. 1

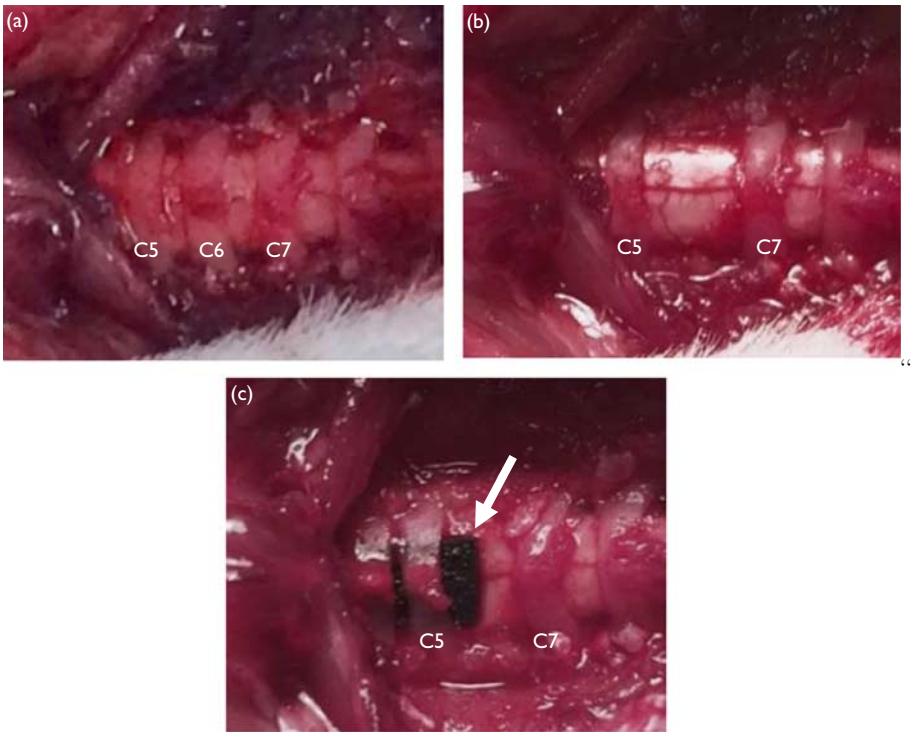

Surgical images showing the process of a water-absorbing polymer sheet implantation. The cervical laminae were exposed (a) and the C6 lamina was removed (b). A water-absorbing polymer sheet (white arrow) was inserted under the C4–C5 laminae (c).

made in the middle of the cervical segments. The C4–C7 laminae were exposed and the C6 lamina was removed. A sheet of water-absorbing polymer was inserted into the C4–C5 sublamina space using a surgical microscope (Fig. 1). We sought to produce an experimental model of myelopathy by static spinal cord compression from the sheet expanding gradually and dynamic compression as a result of flexion and extension of the cervical spine.

Expandable material

We used an expandable sheet made of a water-absorbing polyurethane elastomer. We used Aquaprene Dx (Sanyo Chemical Industries, Kyoto, Japan), which expands in volume by 200%, and Sealer Tape BW (Azuma Gum Industries Company Limited, Gunma, Japan), which expands in volume by 350%. These polymer sheets expand after implantation, absorbing tissue water for 48–72 h to reach their maximum volume. These expandable materials did not show any soft tissue reaction.

Group design

Rats were divided randomly into five experimental groups ($n = 6$ per group) by the expansion rate and thickness of the sheets. Sheets that expanded in volume by 200% (Aquaprene Dx; Sanyo Chemical Industries) were placed in rats in groups 1 (3 mm × 5 mm × 0.5 mm) and 2 (3 mm × 5 mm × 0.7 mm). Sheets that expanded in volume by 350% (Sealer Tape BW; Azuma Gum Industries Company Limited) were placed in rats in groups 3 (3 mm × 5 mm × 0.5 mm) and 4 (3 mm × 5 mm × 0.7 mm). A sheet (3 mm × 5 mm × 0.7 mm) was placed in the C4–C5 sublamina space momentarily in rats in the sham control group and then removed.

Behavioral evaluations

After the surgery, we evaluated the severity of paralysis because of spinal cord compression for 12 weeks. Locomotor function of the forepaws was assessed using a Forelimb Locomotor Scale (FLS) score (0–17 points) [8] and that of the hind paws using a Basso, Beattie, and Bresnahan locomotor rating scale (BBB) score (0–21 points) [9]. Behavioral evaluations were performed before surgery, 1 and 4 days, and 1, 2, 3, 4, 6, 8, 10, and 12 weeks after surgery.

Tissue preparation

Twelve weeks after surgery, the rats were anesthetized with pentobarbital intraperitoneally. Transcardial perfusion with 4% paraformaldehyde in PBS was used to fix tissue. The cervical spine was removed and postfixed in the same fixative overnight and stored in 20% sucrose in PBS at 4°C. The cervical cord was embedded in optimal cutting temperature compound (Sakura Fine Technical, Tokyo, Japan). The cryoprotected samples were frozen at −80°C.

Histology

Transverse sections (10 μm, 10 sections) at the C4/C5 and the C7 segment of the spinal cord were used. These sections at the C4/C5 segment were stained with cresyl violet and sections at the C7 segment were stained with luxol fast blue (LFB). Micrographs were produced using a microscope fitted with a digital camera. The number of motor neurons in the anterior horn at the C4–C5 segment was counted. The LFB-positive area in the corticospinal tract at the C7 segment was calculated. To count motor neurons and calculate the LFB-positive area, we used image analysis software (Image J, version 1.6.0, Rasband WS; US National Institutes of Health, Bethesda, Maryland, USA).

Mechanical testing

We measured Young's modulus of the water-absorbing sheets and spinal cord to determine their hardness using a mechanical testing device. Eight-week-old Sprague-Dawley rats were anesthetized with pentobarbital intraperitoneally and their spinal cords were harvested. C1–C7 laminae were removed. The spinal cord was removed and cut into 5 mm longitudinal samples. Aquaprene Dx (expansion rate: 200%) and Sealer Tape BW (expansion rate 350%) were absorbed with water for a week and maximally expanded. We used spinal cords and four kinds of samples: a sheet with 200% expansion before water absorption, a sheet with 200% expansion after water absorption, a sheet with 350% expansion before water absorption, and a sheet with 350% expansion after water absorption ($n = 3$). The anteroposterior and transverse diameters of each sample were measured using a digital caliper (Digimatic Caliper, Mitutoyo, Japan). Samples were loaded in a mechanical compression testing device (DCS-2000 Universal Testing Machine; Shimadzu Corp., Kyoto, Japan). The actuator was driven at 2 mm/min until 70% strain. The stress–strain curve of each sample was plotted from the results of the compression test. Young's modulus of each sample was identified as the slope of a line tangential to the stress–strain curve [10]. Irreversible neurological deficits have occurred after 30–65% spinal cord compression [1,11,12]. A stress–strain curve for the spinal cord was constructed using the compression test. Young's modulus for the spinal cord at 50–60% strain was measured. Subsequently, we measured Young's modulus for water-absorbing sheets at a stress range of 50–60% strain of the spinal cord.

Statistical analyses

Statistical differences in the FLS score, BBB score, number of motor neurons in the anterior horn, LFB-positive area, and Young's modulus were tested using Turkey's honest significant difference test. P value less than 0.05 was considered significant. Statistical analyses were carried out using the JMP 10 software package (SAS Institute Inc., Cary, North Carolina, USA).

Results

Behavioral evaluations

The BBB score and the FLS score did not change significantly in the control group during 12 weeks postoperatively (Fig. 2). The BBB score and the FLS score decreased at several days postoperatively, but recovered in several weeks in all groups, except for the control group. 'Slow-progressive' paralysis appeared in group 3 (0.5-mm-thick sheet with 200% expansion) at 8 weeks and in group 4 (0.7-mm-thick sheet with 200% expansion) at 4 weeks. At 4 and 6 weeks postoperatively, the average locomotor scores in group 4 were significantly lower than the scores in group 3 ($P < 0.05$). At 12 weeks postoperatively, the average BBB score in group 3 was 10.4 ± 1.2 and the FLS score was 8.8 ± 1.8. The average BBB score in group 4 was 9.0 ± 0.5 and the FLS score was 7.2 ± 0.7. The average locomotor scores in these groups were significantly lower than the scores in group 1 (0.5 mm-thick sheet with 350% expansion), group 2 (0.7 mm-thick sheet with 350% expansion), and the control group ($P < 0.05$). By contrast, from 1 day to 2 weeks postoperatively, fast progressive paralysis was observed and after 3 weeks, recovery from paralysis was observed in groups 1 and 2. At 12 weeks postoperatively, there was no significant difference in the locomotor scores between groups 1, 2, and the control group.

Macroscopic findings

Macroscopic findings at 12 weeks postoperatively showed large erosion of the lamina and mild spinal cord compression despite the considerable swelling of the sheet with 350% expansion (Fig. 3b). By contrast, there was small erosion of the lamina and relatively severe spinal cord compression despite the smaller swelling of the sheet with 200% expansion (Fig. 3c).

Cresyl violet staining

Cavitation and a loss of motor neurons in the anterior horn were observed in all groups, except for the control group (Fig. 4). The number of motor neurons in groups 1–4 was significantly lower than that in the control group ($P < 0.05$).

Luxol fast blue staining

A loss of the LFB-positive area and demyelination in the corticospinal tract were observed in group 3 (0.5-mm-thick sheet with 200% expansion) and group 4 (0.7-mm-thick sheet with 200% expansion) (Fig. 5). By contrast, demyelination was not observed in group 1 (0.5-mm-thick sheet with 350% expansion) or group 2 (0.7-mm-thick sheet with 350% expansion). The LFB-positive area in groups 3 and 4 was significantly lower than that in groups 1, 2, and the control group ($P < 0.05$).

Mechanical testing

A stress–strain curve of the spinal cord was obtained using the compression test (Fig. 6a). From the

Fig. 2

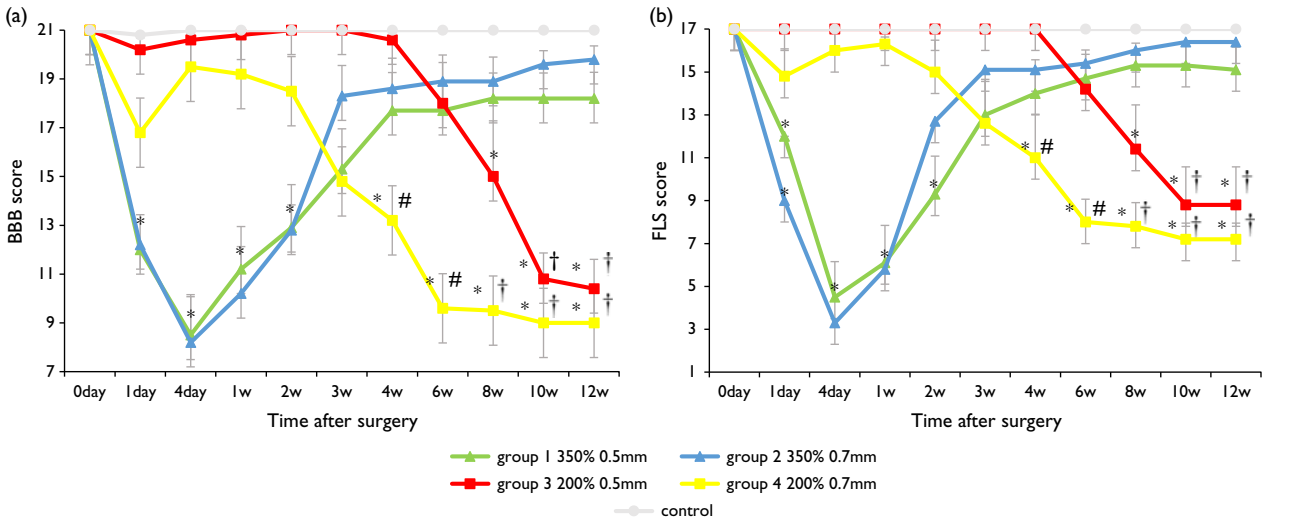

Graphs illustrating Basso, Bieattie, and Bresnahan (BBB) scores (a), and Forelimbs Locomotor Scale (FLS) score (b). BBB and FLS scores of group 3 (expansion rate 200%, thickness 0.5 mm) were significantly lower than those of the control after 8 weeks postoperatively, and that of group 1 or 2 (expansion rate 350%, thickness 0.5 or 0.7 mm) after 10 weeks postoperatively. Similarly, the locomotor score of group 4 (expansion rate 200%, thickness 0.7 mm) was significantly lower than that of the control after 4 weeks postoperatively, and that of group 1 or 2 (expansion rate 350%, thickness 0.5 or 0.7 mm) after 8 weeks postoperatively. There was a significant difference in the locomotor score between group 3 (expansion rate 200%, thickness 0.5 mm) and group 4 (expansion rate 200%, thickness 0.7 mm) after 4 and 6 weeks postoperatively. $^{*}P < 0.05$, significant difference in comparison with the control; $^{\dagger}P < 0.05$, significant difference in comparison with group 1 or 2; $^{\#}P < 0.05$, significant difference in comparison with group 3.

stress–strain curve of the spinal cord, the average stress required for 50% and 60% compression of the spinal cord was 55 ± 9.4 and 172 ± 18 kPa, respectively. The stress–strain curve of each water-absorbing sheet sample was obtained (Fig. 6b) and Young's modulus in the stress range of 50–60% strain of the spinal cord (55–172 kPa) was calculated (Fig. 6c). Young's modulus required for 50–60% compression of the spinal cord was 1130 ± 125 kPa. Young's modulus for the sheet with 350% expansion was 3786 ± 268 kPa before and 1119 ± 26 kPa after water absorption. Young's modulus for the sheet with 200% expansion was 3445 ± 20 kPa before and 2021 ± 93 kPa after water absorption. Young's modulus for the sheet with 200% expansion after water absorption was significantly higher than that for the spinal cord ($P < 0.05$). By contrast, there was no significant difference between Young's modulus for the sheet with 350% expansion after water absorption and that for the spinal cord.

Discussion

This study shows that the polymer sheet with 200% expansion after water absorption was suitable for modeling chronic compressive myelopathy. By contrast, rat models using polymer sheets with 350% expansion reflected temporary and acute myelopathy, which was not suitable to model chronic compressive myelopathy.

In rat models using the sheet with 200% expansion, deterioration occurred temporarily because of surgical invasion, but progressive paralysis occurred after 4–8 weeks postoperatively. Previous reports of a rat model of chronic compressive myelopathy using 3 mm × 5 mm × 0.7 mm water-absorbing sheets with 230% expansion were considered [6,13,14]. Kurokawa *et al.* [13] reported that the ability for treadmill exercise by the rats declined after 6 weeks postoperatively. Yamamoto *et al.* [14] reported that deterioration in grip strength occurred after surgery and recovered in several weeks, and progressive weakness was observed 7–8 weeks postoperatively. In the present study, the results of behavioral evaluations in the groups using sheets with 200% expansion were consistent with these previous reports.

We found loss of motor neurons in the anterior horn and demyelination in the corticospinal tract at 12 weeks postoperatively in rat models using sheets with 200% expansion. Histopathology of cervical spondylotic myelopathy at human autopsy and of rat models showed cavitation and loss of motor neurons in the anterior horn and demyelination in the corticospinal tract [15–17]. Our findings were consistent with these previously reported findings. Therefore, rat models using sheets with 200% expansion reflected slow-progressive myelopathy and were considered to be appropriate as models of chronic compressive myelopathy.

By contrast, temporary paralysis and no demyelination of corticospinal tract at 12 weeks postoperatively were observed in rat models using sheets with 350% expansion after water absorption. These findings were considered to

Fig. 3

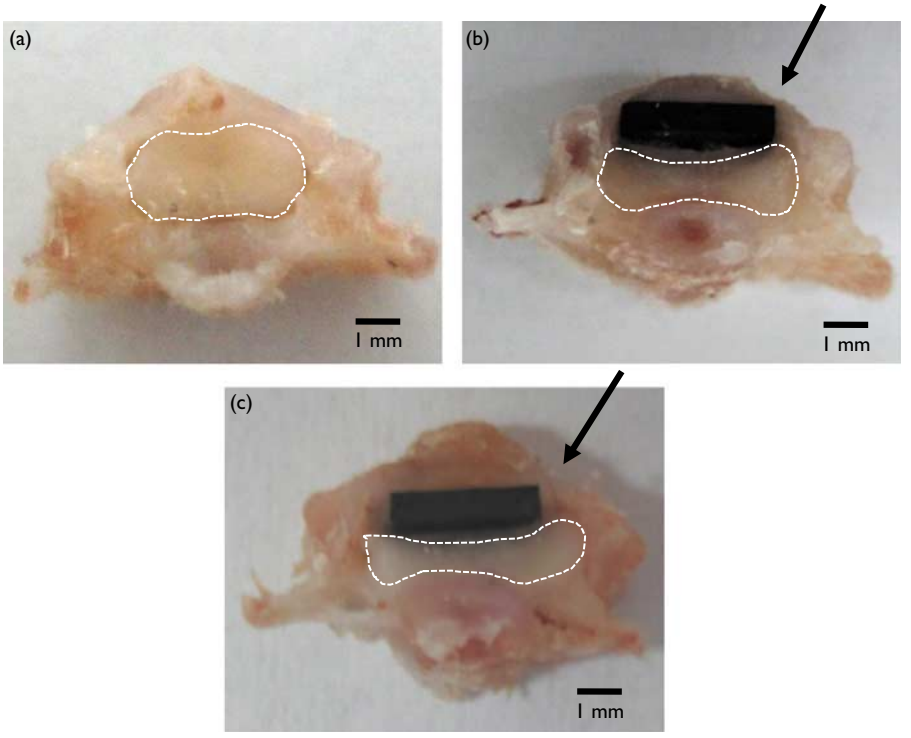

Microimages of the spine of the control group (a), expansion rate 350% and thickness 0.7 mm group (b), and expansion rate 200% and thickness 0.7 mm group, (c) after 12 weeks postoperatively. The erosion of the lamina was large (black arrow) and the spinal cord compression was mild (white dotted line surrounded) despite the large swelling of the sheet with 350% expansion (b). By contrast, the erosion of the lamina was small (black arrow) and spinal cord compression was relatively severe (surrounding white dotted line) despite the small swelling of the sheet with 200% expansion (c).

Fig. 4

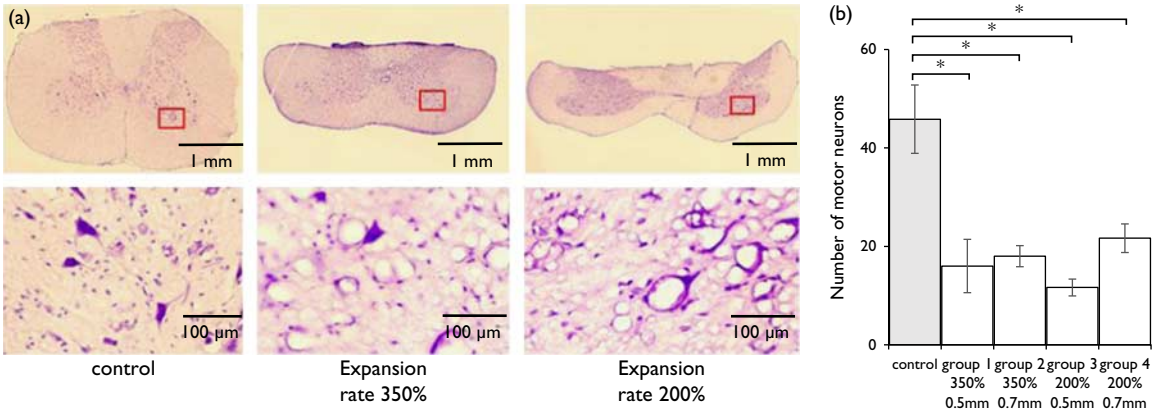

Histological images of cresyl violet staining of the cervical spinal cord at C4/C5 12 weeks postoperatively (a). Bar graph illustrating the number of motor neurons (b). Upper histological images are low magnification. Magnified lower histological images of the area surrounded by a red rectangle in the upper histological images show the anterior horn. Upper images show that the spinal cord is flattened in all groups, except for the control group. Lower images and bar graph show loss of motor neurons in the anterior horn in all groups, except for the control group. $^{*}P < 0.05$, significant difference in comparison with the control.

be acute onset and temporary myelopathy because of surgical invasion and excessive expansion of sheets. Possible reasons for the temporary paralysis and recovery in models using sheets with large expansion are as follows: first, Kim *et al.* [6] reported the reasons for recovery of paralysis in a model of chronic compressive myelopathy, which included a partial reduction of the compression to the spinal cord by erosion and remodeling

Fig. 5

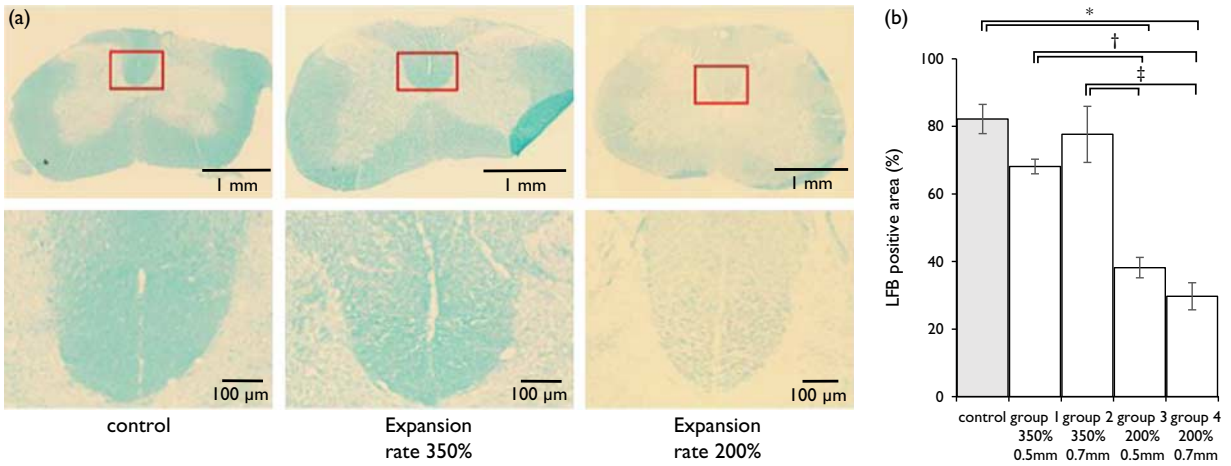

Histological images of luxol fast blue staining of the cervical spinal cord at C7 after 12 weeks postoperatively (a). Bar graph illustrating the percentage of the luxol fast blue-positive area in the corticospinal tract (b). Upper histological images are low magnification. Magnified lower histological images of the area surrounded by a red rectangle in the upper histological images show the corticospinal tract. Histological images and bar graph show that demyelination of the white matter and corticospinal tract are not seen in groups 1, 2, and control. In contrast, demyelination of the white matter and the corticospinal tract are apparent in groups 3 and 4. $^{*}P < 0.05$, significant difference in comparison with the control; $^{\dagger}P < 0.05$, significant difference in comparison with group 1; $^{\ddagger}P < 0.05$, significant difference in comparison with group 2.

Fig. 6

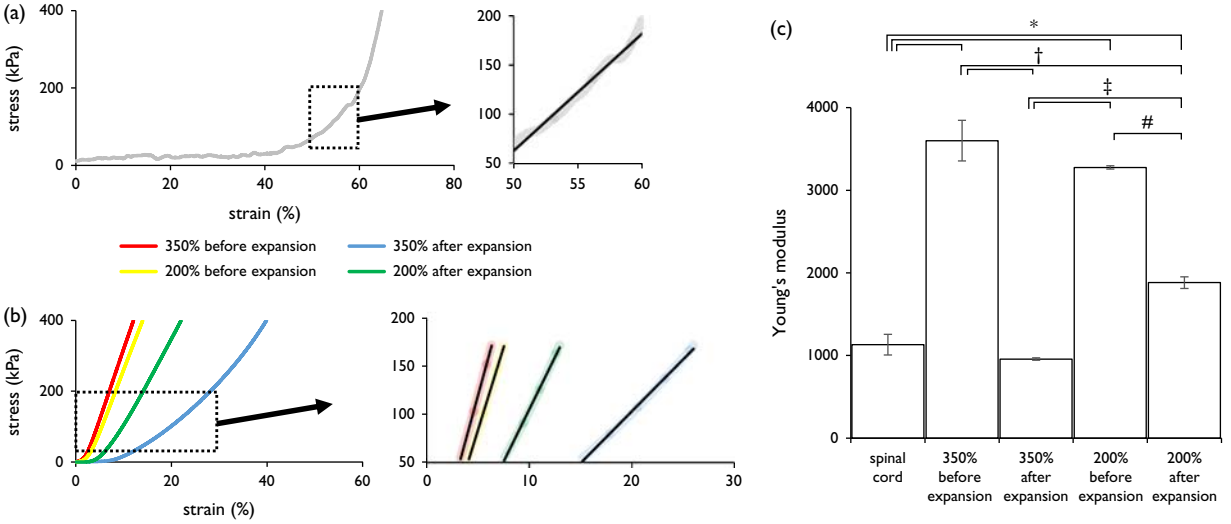

The sample of the stress–strain curve (left) and the tangential line (right) of the spinal cord (a) and water-absorbing sheets (b). Young's modulus of water-absorbing sheets and the spinal cord (c). $^{*}P < 0.05$, significant difference in comparison with the spinal cord; $^{\dagger}P < 0.05$, significant difference in comparison with the sheet with 350% expansion before water absorption; $^{\ddagger}P < 0.05$, significant difference in comparison with the sheet with 350% expansion after water absorption; $^{\#}P < 0.05$, significant difference in comparison with the sheet with 200% expansion before water absorption.

of the lamina overlying the polymer sheet. Another reason might be related to the hardness of the water-absorbing sheet after expansion. Mechanical testing showed that the sheet with 200% expansion after water absorption was harder than the spinal cord, but the sheet with 350% expansion after water absorption was not. Therefore, paralysis might have been temporary and recovered in models using sheets with 350% expansion because the sheet with 350% expansion after water absorption was not harder than the spinal cord. Paralysis might be slowly progressive in models using sheets with 200% expansion because the sheets with 200% expansion are harder than the spinal cord.

The behavioral results for the models using sheets with 200% expansion were an earlier appearance of paralysis in

the subgroup of models using 0.7-mm-thick sheets than in the subgroup using 0.5-mm-thick sheets. However, temporary paralysis after surgery because of surgical invasion was greater in the subgroup of models using 0.7-mm-thick sheets. If the thickness of the sheet is more than 0.7 mm, invasion is even greater and the risk of iatrogenic spinal cord injury increases. In the unpublished data from preliminary experiments, spinal cord injury frequently occurred after inserting 1.0-mm-thick sheets under the laminae. Kubota *et al.* [18] reported a mouse model of subclinical spinal canal stenosis. The mouse model had no paralysis for 6 weeks after a 300-μm-thick sheet was inserted under the laminae. If the thickness of the sheet was less than 0.3 mm, the probability of paralysis was considerably less. Therefore, a thickness of 0.5–0.7 mm was considered suitable for rat models of chronic compressive myelopathy.

An animal model of CCM using a chronic compression device [19], and flat plastic screw implantation through spinal lamina [20], showed acute paralysis or progressive recovery several weeks after surgery. Long *et al.* [7] used a water-absorbing sheet with 700% expansion. However, their observation period was only 1 week and insufficient for chronic compressive myelopathy. These models did not reflect 'chronic' or 'slow-progressive' myelopathy. We considered that delayed and slow-progressive paralysis was necessary to model chronic compressive myelopathy.

Limitations

Spondylosis and the dynamic factor were not considered in the present study. To reflect the pathophysiology of CCM of humans, it is necessary to develop a compressive myelopathy model that takes these factors into consideration.

Conclusion

A polymer sheet that expands in volume by 200% after water absorption is an ideal material for rat models of CCM. The hardness of the material inserted under the spinal lamina is important to reflect chronic compressive myelopathy.

Acknowledgements

This work was supported by grants-in-aid for Scientific Research from the Ministry of Education, Science and Culture of Japan (15561169).

Conflicts of interest

There are no conflicts of interest.

References

1 Fehlings MG, Skaf G. A review of the pathophysiology of cervical spondylotic myelopathy with insights for potential novel mechanisms drawn from traumatic spinal cord injury. *Spine* 1998; **23**:2730–2737.
2 Bohlman HH, Emery SE. The pathophysiology of cervical spondylosis and myelopathy. *Spine* 1988; **13**:843–846.
3 Panjabi M, White A 3rd. Biomechanics of nonacute cervical spinal cord trauma. *Spine* 1988; **13**:838–842.
4 Kalsi-Ryan S, Karadimas SK, Fehlings MG. Cervical spondylotic myelopathy: the clinical phenomenon and the current pathobiology of an increasingly prevalent and devastating disorder. *Neuroscientist* 2013; **19**:409–421.
5 Khuyagbaatar B, Kim K, Kim YH. Conversion equation between the Drop Height in the New York University Impactor and the Impact Force in the Infinite Horizon Impactor in the Contusion Spinal Cord Injury Model. *J Neurotrauma* 2015; **32**:1987–1993.
6 Kim P, Haisa T, Kawamoto T, Kirino T, Wakai S. Delayed myelopathy induced by chronic compression in the rat spinal cord. *Ann Neurol* 2004; **55**:503–511.
7 Long HQ, Li GS, Lin EJ, Xie WH, Chen WL, Luk KD, Hu Y. Is the speed of chronic compression an important factor for chronic spinal cord injury rat model? *Neurosci Lett* 2013; **545**:75–80.
8 Cao Y, Shumsky JS, Sabol MA, Kushner RA, Strittmatter S, Hamers FP, *et al.* Nogo-66 receptor antagonist peptide (NEP1-40) administration promotes functional recovery and axonal growth after lateral funiculus injury in the adult rat. *Neurorehabil Neural Repair* 2008; **22**:262–278.
9 Basso DM, Beattie MS, Bresnahan JC. A sensitive and reliable locomotor rating scale for open field testing in rats. *J Neurotrauma* 1995; **12**:1–21.
10 Bosisio MR, Talmant M, Skalli W, Laugier P, Mitton D. Apparent Young's modulus of human radius using inverse finite-element method. *J Biomech* 2007; **40**:2022–2028.
11 Ichihara K, Taguchi T, Shimada Y, Sakuramoto I, Kawano S, Kawai S. Gray matter of the bovine cervical spinal cord is mechanically more rigid and fragile than the white matter. *J Neurotrauma* 2001; **18**:361–367.
12 Galle B, Ouyang H, Shi R, Nauman E. Correlations between tissue-level stresses and strains and cellular damage within the guinea pig spinal cord white matter. *J Biomech* 2007; **40**:3029–3033.
13 Kurokawa R, Nagayama E, Murata H, Kim P. Limaprost alfadex, a prostaglandin E1 derivative, prevents deterioration of forced exercise capability in rats with chronic compression of the spinal cord. *Spine* 2011; **36**:865–869.
14 Yamamoto S, Kurokawa R, Kim P. Cilostazol, a selective type III phosphodiesterase inhibitor: prevention of cervical myelopathy in a rat chronic compression model. *J Neurosurg Spine* 2014; **20**:93–101.
15 Karadimas SK, Moon ES, Yu WR, Satkunendrarajah K, Kallitsis JK, Gatzounis G, Fehlings MG. A novel experimental model of cervical spondylotic myelopathy (CSM) to facilitate translational research. *Neurobiol Dis* 2013; **54**:43–58.
16 Mizuno J, Nakagawa H, Chang HS, Hashizume Y. Postmortem study of the spinal cord showing snake-eyes appearance due to damage by ossification of the posterior longitudinal ligament and kyphotic deformity. *Spinal Cord* 2005; **43**:503–507.
17 Kameyama T, Hashizume Y, Ando T, Takahashi A, Yanagi T, Mizuno J. Spinal cord morphology and pathology in ossification of the posterior longitudinal ligament. *Brain* 1995; **118** (**Pt 1**):263–278.
18 Kubota K, Saiwai H, Kumamaru H, Kobayakawa K, Maeda T, Matsumoto Y, *et al.* Neurological recovery is impaired by concurrent but not by asymptomatic pre-existing spinal cord compression after traumatic spinal cord injury. *Spine*, **37**:1448–1455.
19 Lee J, Satkunendrarajah K, Fehlings MG. Development and characterization of a novel rat model of cervical spondylotic myelopathy: the impact of chronic cord compression on clinical, neuroanatomical, and neurophysiological outcomes. *J Neurotrauma* 2012; **29**:1012–1027.
20 Sun Y, Zhang LH, Fu YM, Li ZR, Liu JH, Peng J, *et al.* Establishment of a rat model of chronic thoracolumbar cord compression with a flat plastic screw. *Neural Regen Res* 2016; **11**:963–970.